Membrane cholesterol modulates the hyaluronan-binding ability of CD44 in T lymphocytes and controls rolling under shear flow

Toshiyuki Murai[1,*], Chikara Sato[2,3], Mari Sato[2], Hidetoshi Nishiyama[4], Mitsuo Suga[4], Kazuhiro Mio[2,3] and Hiroto Kawashima[5]

[1]Department of Microbiology and Immunology, Graduate School of Medicine, Osaka University, Suita, Osaka 565-0871, Japan
[2]Biomedical Research Institute, National Institute of Advanced Industrial Science and Technology (AIST), Tsukuba, Ibaraki 305-8568, Japan
[3]Biomedicinal Information Research Center, National Institute of Advanced Industrial Science and Technology (AIST), Tokyo 135-0064, Japan
[4]Advanced Technology Division, JEOL Ltd., Akishima, Tokyo 196-8558, Japan
[5]Laboratory of Microbiology and Immunology, School of Pharmaceutical Sciences, University of Shizuoka, Shizuoka 422-8526, Japan
*Author for correspondence (murai@orgctl.med.osaka-u.ac.jp)

Accepted 10 May 2013
Journal of Cell Science 126, 3284–3294

doi: 10.1242/jcs.120014

Summary

The adhesion of circulating lymphocytes to the surface of vascular endothelial cells is important for their recruitment from blood to secondary lymphoid organs and to inflammatory sites. CD44 is a key adhesion molecule for this interaction and its ligand-binding ability is tightly regulated. Here we show that the hyaluronan-binding ability of CD44 in T cells is upregulated by the depletion of membrane cholesterol with methyl-β-cyclodextrin (MβCD), which disintegrates lipid rafts, i.e. cholesterol- and sphingolipid-enriched membrane microdomains. Increasing concentrations of MβCD led to a dose-dependent decrease in cellular cholesterol content and to upregulation of hyaluronan binding. Additionally, a cholesterol-binding agent filipin also increased hyaluronan binding. Cholesterol depletion caused CD44 to be dispersed from cholesterol-enriched membrane microdomains. Cholesterol depletion also increased the number of cells undergoing rolling adhesion under physiological flow conditions. Our results suggest that the ligand-binding ability of CD44 is governed by its cholesterol-dependent allocation to membrane microdomains at the cell surface. These findings provide novel insight into the regulation of T cell adhesion under blood flow.

Key words: Adhesion molecule, Cholesterol, Hyaluronan, Lipid raft

Introduction

Lymphocyte recruitment from circulating blood to secondary lymphoid organs and to inflammatory sites takes place through complementary receptor–ligand interactions between lymphocytes and vascular endothelial cells. Recognition of the endothelial surface by circulating lymphocytes and their subsequent extravasation occur through a multistep series of sequential receptor engagements (Springer, 1994). This process begins with the establishment of transient adhesive interactions that result in the rolling of lymphocytes along the endothelium under blood flow. This rolling adhesion is prerequisite for the subsequent firm adhesion of lymphocytes to the endothelium and transmigration across blood vessels, and the roles of selectins and their sulfated glycan ligands in rolling adhesion have been well investigated (Rosen, 2004; Kawashima et al., 2005; Kawashima, 2006). The rolling is also mediated by the interactions between the transmembrane adhesion receptor CD44 and its glycan ligand: CD44 on T cells mediates the rolling of T cells on the extracellular matrix component hyaluronan (HA), a linear glycosaminoglycan composed of D-glucuronic acid and *N*-acetyl-D-glucosamine repeats, *in vitro* (DeGrendele et al., 1996; Clark et al., 1996). The CD44–HA interaction also mediates T cell rolling *in vivo* (Bonder et al., 2006), and is required in the extravasation of activated T cells from circulating blood to inflammatory sites (DeGrendele et al., 1997). There is also evidence that the homing of $CD4^+CD25^+$ regulatory T cells (T_{reg} cells) to nasal-associated lymphoid tissues (NALTs) is partially dependent on CD44 (Ohmichi et al., 2011).

Although CD44 is the principal receptor for HA in immune cells, the majority of immune cells express CD44 that does not bind HA constitutively (Lesley et al., 1993). Considering the ubiquitous distribution of CD44 and HA, tight regulation of the HA-binding ability of CD44 is likely to play a critical role in immunological responses. In fact, CD44 on resting T cells does not bind HA, but can be induced to bind it upon T cell activation with antigen via the T cell receptor (TCR) (DeGrendele et al., 1997; Lesley et al., 1994; Ariel et al., 2000; Firan et al., 2006; Maeshima et al., 2011). Studies report that various post-translational modifications on CD44, including glycosylation (Katoh et al., 1995; English et al., 1998; Skelton et al., 1998), chondroitin sulfate addition (Levesque and Haynes, 1999; Ruffell et al., 2011), and sulfation (Maiti et al., 1998; Brown et al., 2001), affect its HA-binding ability. However, the membrane-based regulation of CD44's HA-binding ability has not been clarified.

Much attention has recently been paid to the role of lipid rafts, cholesterol- and glycosphingolipid-enriched membrane microdomains (Simons and Ikonen, 1997; Fessler and Parks, 2011). Lipid rafts at the cell surface serve as platforms for signaling molecules such as

Src family protein kinases, G-proteins and adaptor proteins. Although the CD44 in T cells is associated with lipid rafts (Ilangumaran et al., 1998; Gómez-Móuton et al., 2001), the functional significance of this localization has been largely unknown.

In the present study, we demonstrate that the HA-binding ability of CD44 in T cells is upregulated by membrane cholesterol depletion, which causes CD44 to be dispersed from cholesterol-enriched membrane microdomains. Cholesterol depletion also enhanced the frequency of rolling adhesion under physiological flow conditions. Our results suggest that CD44's ligand-binding ability is governed by the cholesterol-dependent localization of CD44 to membrane microdomains at the cell surface.

Results

MβCD upregulates the HA-binding ability of CD44

To study whether the cholesterol-enriched membrane microdomains, i.e. lipid rafts, modulate CD44 activity, we examined the HA-binding ability of a mouse T cell line BW5147, which expresses functional CD44 that mediates rolling adhesion on glycosaminoglycans including HA (Murai et al., 2004a). Flow cytometric analysis using 2 μg/ml FITC-conjugated HA (FITC–HA; 180 kDa) showed that BW5147 T cells expressed CD44 abundantly and bound FITC–HA (supplementary material Fig. S1). PMA treatment (10 ng/ml for 16 hours) upregulated the HA-binding ability in agreement with previous reports (DeGrendele et al., 1996; Liu and Sy, 1997). Next, to study whether lipid rafts modulate CD44 activity, we treated BW5147 T cells with the cholesterol-binding agent methyl-β-cyclodextrin (MβCD), and performed the flow cytometric analysis. Since MβCD selectively extracts the membrane cholesterol that maintains the assembled structures of lipid rafts, it is frequently used to disrupt them (Ilangumaran and Hoessli, 1998). BW5147 T cells treated with 0, 2.5 and 5 mM MβCD for 1 hour showed a concentration-dependent increase in the HA-binding (Fig. 1A), which was negatively correlated with the cellular cholesterol content (Fig. 1B). Incubation with 5 mM MβCD for 1 hour reduced cholesterol levels by around 40% (Fig. 1B), but retained cell viability and shape (data not shown), although incubation with 10 mM MβCD for 1 hour did compromise cell viability (data not shown). Flow cytometric analyses using FITC–HA with different molecular mass (29 kDa and 1300 kDa) or at much higher concentration (50 μg/ml) exhibited similar shift in HA-binding (supplementary material Fig. S2). Pretreatment of BW5147 T cells with a PKC inhibitor GF109203X did not inhibit the upregulation of HA-binding ability upon MβCD (supplementary material Fig. S3), suggesting that cholesterol manipulation and PMA modulate the HA-binding ability of CD44 through different mechanisms. Next, we examined the effect of incubating cells with 5 mM MβCD from 0.5 to 1.5 hours, and found no marked difference in the HA-binding ability and cellular cholesterol levels over this interval (Fig. 1C,D). Therefore, we performed the following experiments with 5 mM MβCD and a 1-hour incubation.

Because cholesterol depletion can inhibit clathrin-dependent endocytosis (Rodal et al., 1999), one possible explanation for the increased HA-binding was an increase in the amount of CD44 at the cell surface. However, MβCD treatment did not alter the cell-surface level of CD44 (Fig. 1E), and the binding of FITC–HA to BW5147 T cells was completely inhibited by the anti-CD44 blocking mAb KM201 (Fig. 1F), confirming that the binding was mediated by surface CD44. It was recently reported that cancer cells shed a portion of their surface CD44 during incubation with MβCD (Murai et al., 2011). To examine whether the CD44 on BW5147 T cells was shed upon MβCD treatment, we immunoprecipitated CD44 from the culture supernatants using the anti-CD44 mAb IM7, but no detectable soluble CD44 was found after MβCD treatment (supplementary material Fig. S4). In addition, the surface CD44 level was not changed by the presence of a hydroxamate-based metalloproteinase inhibitor TAPI (tumor necrosis factor-α protease inhibitor) (supplementary material Fig. S5), which inhibits the shedding of CD44 from cancer cells (Murai et al., 2011). These results indicate that BW5147 T cells do not intensely shed surface CD44 upon MβCD treatment.

Cholesterol manipulation alters the HA-binding ability of CD44

To verify that cholesterol modulates the HA-binding ability of CD44, we replenished the cholesterol in cholesterol-depleted cells using a cholesterol–MβCD inclusion complex, as described previously (Klein et al., 1995). This treatment reduced the HA-binding ability induced by MβCD to the basal level, while surface level of CD44 was slightly changed (Fig. 2A). Thus, the increase in the HA-binding ability of CD44 upon MβCD treatment was due to the depletion of cellular cholesterol, and was reversed when the cholesterol was replenished. We also tested the effect of cholesterol reduction by enzymatic oxidation. The cell-impermeable enzyme cholesterol oxidase converts cholesterol to cholestenone, and is widely used to manipulate plasma membrane cholesterol to achieve a modest decrease in the cholesterol and protein content of detergent-resistant membranes (DRMs) (Le Lay et al., 2009). The incubation of BW5147 T cells with cholesterol oxidase (0.5 U/ml for 1 hour) caused a slight increase in the HA-binding ability of CD44, and it did not alter the cell-surface level of CD44 (Fig. 2B).

Next, we perturbed lipid raft integrity by another method, cholesterol sequestration by the polyene macrolide antibiotic filipin. Filipin binds cholesterol and disperses it in the membrane; it is used in lipid raft research as an agent that sequesters cholesterol in lipid rafts, thereby disrupting them (McGookey et al., 1983; Rothberg et al., 1990). As shown in Fig. 2C, filipin (2 μg/ml for 1 hour) increased the HA-binding ability of CD44, although much less than MβCD. These results suggest that the cholesterol-rich lipid rafts are involved in the regulation of HA-binding by CD44.

Cholesterol depletion causes CD44 to be dispersed from detergent-insoluble membrane compartments

We examined whether the partitioning of CD44 between lipid rafts and non-raft regions in BW5147 T cells is influenced by the manipulation of cholesterol with MβCD that modulated the HA-binding ability of CD44, using biochemical ultracentrifugation analysis and immunoelectron microscopy. Lipid rafts can be fractionated as DRM complexes using a nonionic detergent such as Triton X-100 (Simons and Ikonen, 1997). BW5147 T cells were treated with MβCD (5 mM) or left untreated for 1 hour, lysed with Triton X-100, and subjected to gradient centrifugation analysis. As shown in Fig. 3, a small fraction of the CD44 in untreated BW5147 T cells was found in the low-density fraction, in agreement with a previous report (Gómez-Móuton et al., 2001). However, some CD44 was clearly lost from the Triton X-100-insoluble fraction after cholesterol depletion with MβCD.

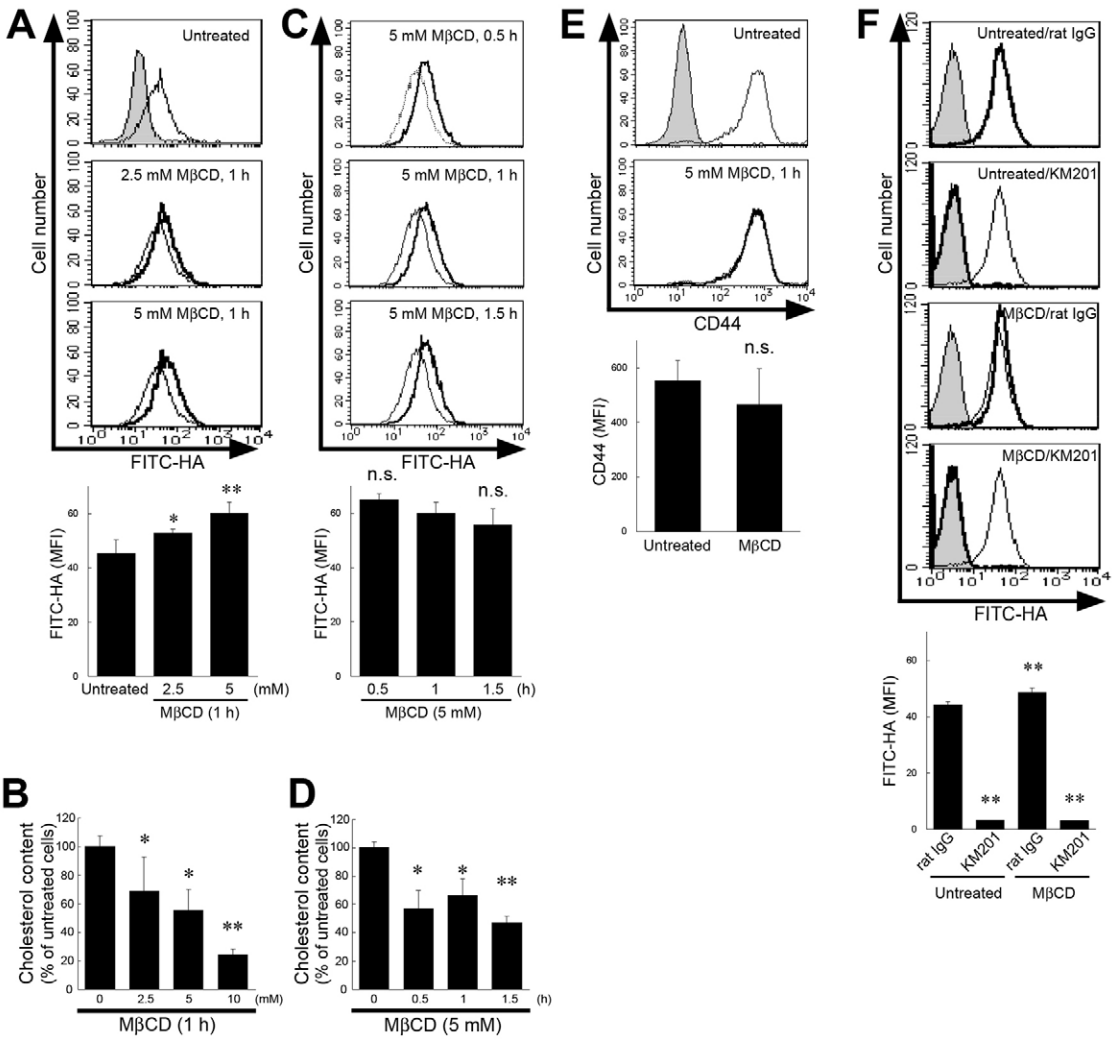

Fig. 1. MβCD enhances the HA-binding ability of CD44. (**A**) Dose-dependent effect of MβCD on HA binding. BW5147 T cells were treated with 2.5 or 5 mM MβCD (thick lines) or left untreated (thin lines) for 1 hour at 37℃. The extent of FITC–HA binding was determined by flow cytometry. Bar graphs show levels of FITC–HA binding as quantified by mean fluorescence intensity (MFI) of each profile. Data are presented as mean ± s.d. of triplicate determination (ANOVA/Dunnett's test). Gray-filled profile, unstained control. (**B**) Changes in the cellular cholesterol content after treatment with various concentrations (0, 2.5, 5 and 10 mM) of MβCD for 1 hour (ANOVA/Dunnett's test). (**C**) Time course of the effect of MβCD on HA binding. Cells were treated with 5 mM MβCD for 0.5, 1 or 1.5 hours (thick lines) or left untreated (thin lines). FITC–HA binding was determined by flow cytometry. Bar graphs show quantification of MFI for FITC–HA binding. Results were compared with the 1-hour treatment (ANOVA/Dunnett's test). (**D**) Changes in the cellular cholesterol content after treatment with 5 mM MβCD for 0, 0.5, 1 and 1.5 hours (ANOVA/Dunnett's test). (**E**) Effect of MβCD on the cell-surface level of CD44. Cells were treated with 5 mM MβCD for 1 hour (thick line) or left untreated (thin lines). Binding of anti-CD44 mAb IM7 was determined by flow cytometry. Gray-filled profile, isotype-matched control. Bar graphs show quantification of MFI for CD44 (Student's *t*-test). (**F**) Effect of anti-CD44 blocking mAb on HA binding. Cells were treated with 5 mM MβCD or left untreated for 1 hour. The cells were then left untreated (thin lines) or incubated with either 10 μg/ml anti-CD44 blocking mAb KM201 or normal rat IgG (thick lines) for 30 minutes. The binding of FITC–HA was determined by flow cytometry. Gray-filled profiles, unstained control. Bar graphs show quantification of MFI for FITC–HA binding (ANOVA/Dunnett's test). n.s., not significant, $*P<0.05$, $**P<0.01$ compared with the corresponding control.

Next we attempted to observe the distribution of CD44 on the plasma membrane, and how it is changed by raft disruption, using atmospheric scanning electron microscope (ASEM). The ASEM enables direct observation of subcellular structures and the localization of proteins of interest in wet cells at SEM resolution (Murai et al., 2011). The observable specimen thickness is 2–3 μm from the silicon nitride (SiN) film (Nishiyama et al., 2010). We labeled CD44 on the cell surface of MβCD-treated or untreated cells with Nanogold, followed by gold enhancement. ASEM observation revealed that CD44 was localized over the entire cell surface including the cell body and the microvilli, and that CD44 clustering was disordered after cholesterol depletion (Fig. 4). The clustered particles formed agglomerations of gold signals of 100–300 nm in size in the untreated cells (Fig. 4A; Fig. 4A1–A5) as indicated by arrow heads in Fig. 4A4, while they were dissociated in the cells treated with 5 mM MβCD (Fig. 4B; Fig. 4B1–B5).

Johnson and others have intensively investigated the regulation of CD44 function, and shown that post-translational modifications to CD44 are implicated in modulating its HA-binding ability (Katoh et al., 1995; English et al., 1998; Skelton et al., 1998; Levesque and Haynes, 1999; Ruffell et al., 2011; Maiti et al., 1998; Brown et al., 2001). Under the conditions described here, however,

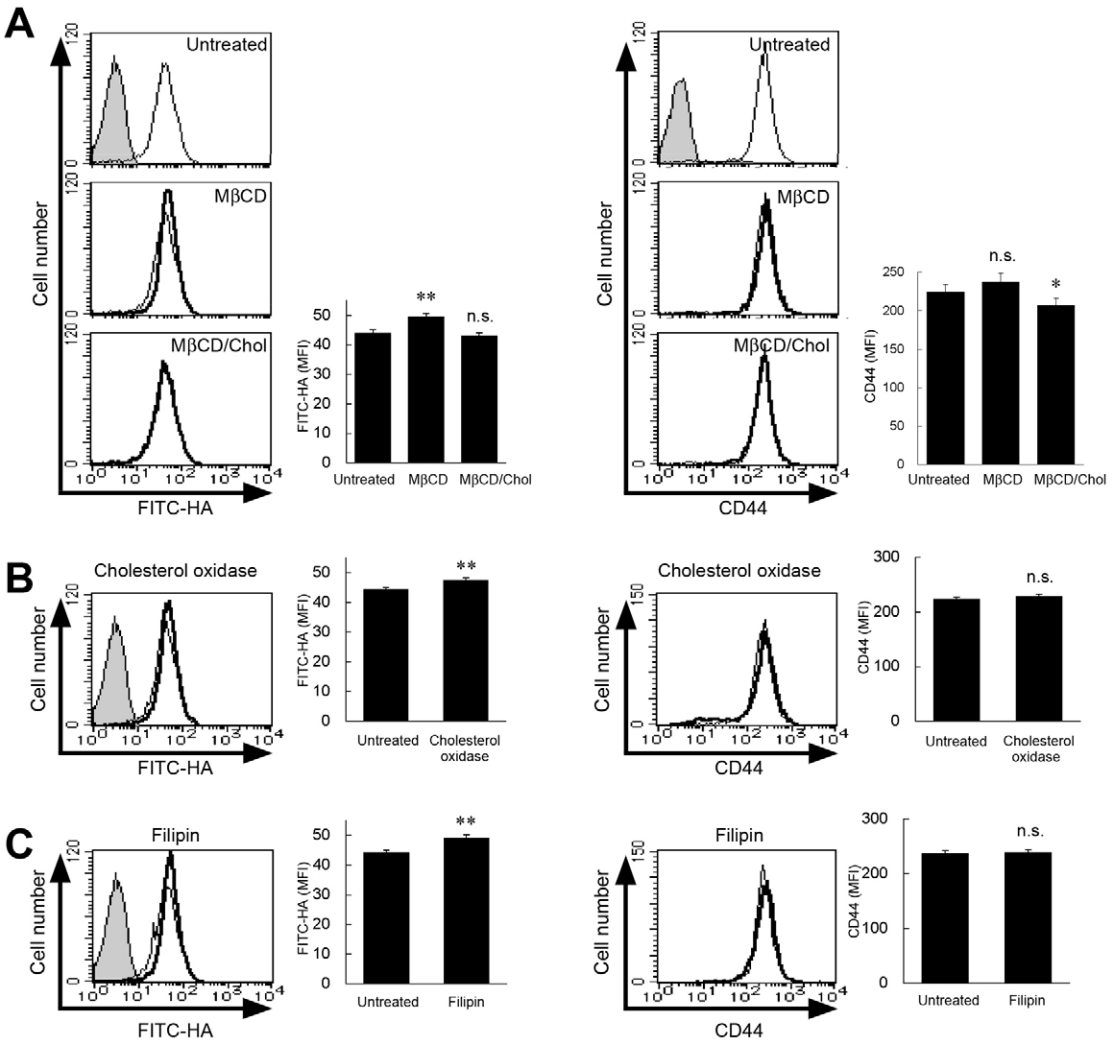

Fig. 2. Manipulation of membrane cholesterol alters the HA-binding ability of CD44. (**A**) Effect of cholesterol replenishment on the HA-binding ability of CD44. Unstimulated BW5147 T cells (upper graphs) were treated with 5 mM MβCD for 1 hour (middle graphs), and subsequently treated with 0.3 mM cholesterol-3 mM MβCD complex for 30 minutes (lower graphs). At every step, the binding of FITC–HA (left) and the level of cell surface CD44 (right) were determined by flow cytometry. Thick lines, treated cells; thin lines, untreated cells; gray-filled profiles, staining control. Bar graphs show quantification of MFI for FITC-HA binding (left) and CD44 (right) (ANOVA/Dunnett's test). (**B**) Effect of cholesterol oxidation on the HA-binding ability of CD44. BW5147 T cells were treated with 0.5 U/ml cholesterol oxidase (thick lines) or left untreated (thin lines) for 1 hour at 37℃. The binding of FITC–HA (left) and the CD44 level (right) were determined by flow cytometry. Gray-filled profile, staining control. Bar graphs show quantification of MFI for FITC-HA (left) and CD44 (right) (Student's *t*-test). (**C**) Effect of filipin on the HA-binding ability of CD44. BW5147 T cells were treated with 2 μg/ml filipin (thick lines) or left untreated (thin lines) for 1 hour at 37℃. Binding of FITC–HA (left) and the CD44 level (right) were determined by flow cytometry. Gray-filled profile, staining control. Bar graphs show quantification of MFI for FITC–HA binding (left) and CD44 (right) (Student's *t*-test). n.s., not significant, $*P<0.05$,$**P<0.01$ versus untreated cells.

the involvement of post-translational modifications may not matter, since the HA-binding ability of CD44 rose within 30 minutes (Fig. 1). It is also reported that the HA-binding ability of CD44 is upregulated upon PMA stimulation in Jurkat human T cells, as a result of activation-induced CD44 dimerization, which is mediated by a disulfide bond (Liu and Sy, 1997). We therefore investigated whether this dimerization was involved in the increase in the HA-binding ability after cholesterol manipulation. After cholesterol depletion, BW5147 T cells were surface-biotinylated, lysed, immunoprecipitated with an anti-CD44 mAb, and subjected to non-reducing PAGE followed by western blotting. However, no detectable band corresponding to the dimer was observed (supplementary material Fig. S6A).

Cholesterol depletion alters the cell adhesion properties

We examined whether cholesterol manipulation can modulate the cell adhesion mediated by CD44 and HA. As shown in Fig. 5, the incubation of BW5147 T cells with MβCD significantly enhanced cell adhesion to HA-coated microtiter plates. Cholesterol replenishment using the cholesterol–MβCD complex reduced cell adhesion to the basal level, confirming the specificity of MβCD. Filipin did not show significant effects on static cell binding. Incubation with anti-CD44 blocking mAb KM201 (shown by + in Fig. 5) inhibited cell adhesion in every case. These results indicate that cholesterol depletion enhanced cell adhesion that was mediated by cell-surface CD44 and immobilized HA.

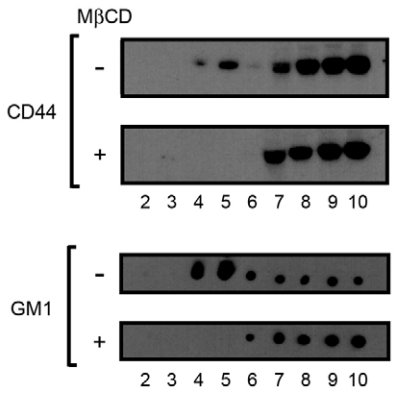

Fig. 3. Cholesterol depletion causes the dispersion of CD44 from lipid rafts. BW5147 T cells treated with MβCD (5 mM, 1 hour) or left untreated were lysed in TNE buffer containing 0.5% Triton X-100 and the lysate subjected to gradient centrifugation as described in Materials and Methods. Each fraction was analyzed by western blotting. The lipid raft marker GM1 was detected by dot blot analysis using biotinylated CTxB and HRP-conjugated streptavidin.

We next studied the effect of cholesterol manipulation on CD44-dependent rolling under flow conditions. BW5147 T cells exhibited rolling on HA under physiological flow conditions (Fig. 6Aa,Ab). Rolling cells were easily distinguished by these prominent features: they showed low velocity compared to the non-interacting cells, with an irregular jerky rolling motion, with which they appeared to detach and attach briefly to the capillary wall. Cells that were non-adherent and floating were not observed, due to their high velocity. There were no statically attached cells. When the BW5147 T cells were treated with MβCD (5 mM for 1 hour), the frequency of rolling cells increased at wall shear stresses of 0.4 and 0.8 dyn/cm^2 (Fig. 6Ad), while the average rolling velocity did not change (Fig. 6Ac). Cholesterol replenishment of the MβCD-treated cells reduced the frequency of rolling cells to the basal level, with unchanged average velocity, confirming the specificity of MβCD (Fig. 6Ae,Af). Filipin treatment had no marked effect on either the rolling velocity or frequency (Fig. 6Ag,Ah), suggesting that the effectiveness of filipin and MβCD on raft disruption might be different among cells, i.e. filipin showed raft-disruption effects to the same extent as MβCD in glioma cells (Murai et al., 2011) and milder effects in hematopoietic cells, considering the fact that the effects of filipin were significant but not very dramatic on BW5147 T cell's HA binding determined by FACS (Fig. 2C). These results indicate that cholesterol depletion enhances the rolling of BW5147 T cells, and suggest that lipid rafts may control T cell rolling by modulating the HA-binding ability of CD44.

Next, we evaluated the functional consequences of MβCD-enhanced HA-binding on interactions of BW5147 T cells with endothelial cells. We used the mouse lymph node endothelial cell SVEC4-10 for this study, because SVEC4-10 cells express abundant HA on their cell surface, which supports CD44-mediated cell rolling under physiological flow condition (DeGrendele et al., 1996). Untreated BW5147 T cells exhibited rolling adhesion at wall shear stress of 0.4 dyn/cm^2, and the frequency of rolling cells increased when cells were treated with MβCD (5 mM for 1 hour) (Fig. 6Bb), while the average rolling

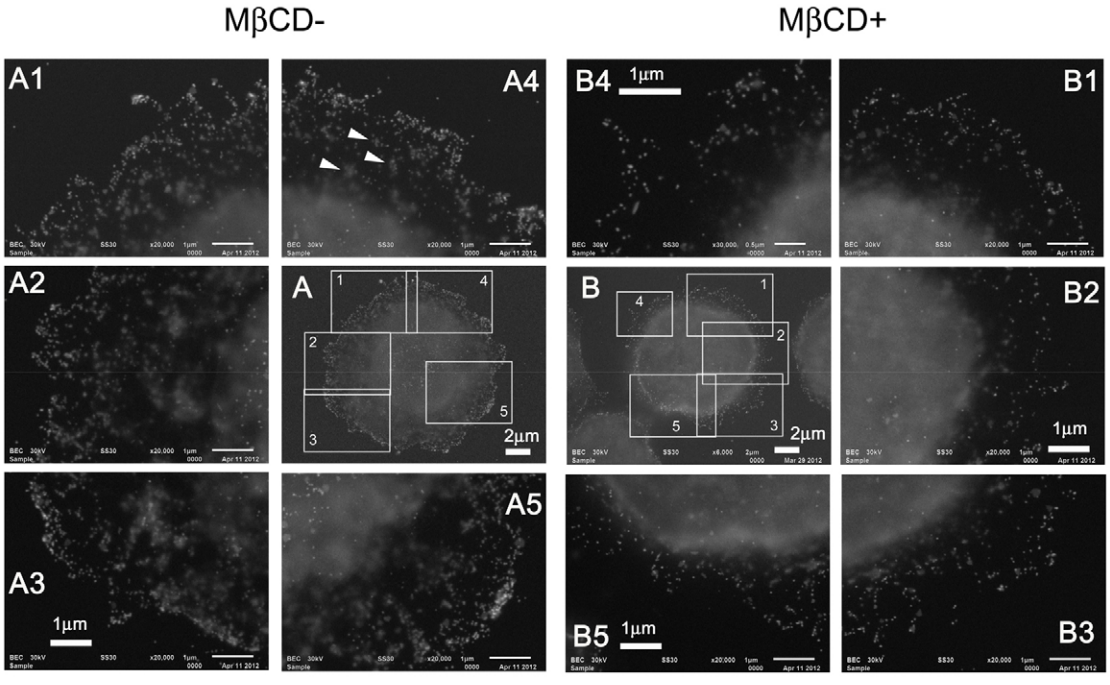

Fig. 4. ASEM observation of CD44 distribution on the plasma membrane. (A,B) BW5147 T cells were left untreated (A) or treated with 5 mM MβCD for 1 hour (B) and then fixed with 4% paraformaldehyde. To detect CD44 on the cell surface, the cells were incubated with anti-CD44 mAb IM7, then with Alexa Fluor 488- and Nanogold (1.4 nm)-conjugated goat anti-rat IgG, followed by gold enhancement. The labeled cells were observed using ASEM at 6000× (A,B), 20,000× (A1–A5, B1–B3, B5) and at 30,000× (B4) magnification. Agglomerations of gold signals (arrowheads) were observed on the untreated cells. Scales are indicated by the thick bars.

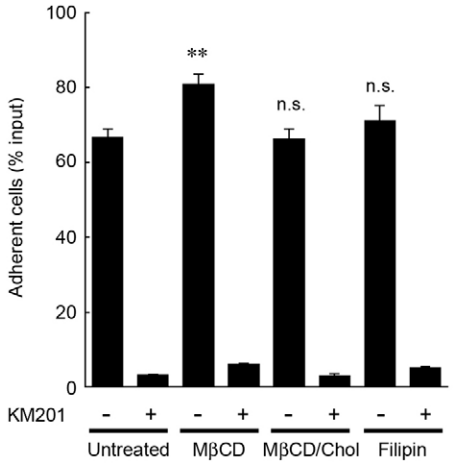

Fig. 5. Cholesterol depletion upregulates cell adhesion to HA under static conditions. CMFDA-labeled BW5147 T cells were left untreated, MβCD-treated (5 mM for 1 hour), cholesterol-replenished (MβCD/Chol) or filipin-treated (2 μg/ml for 1 hour), and subsequently incubated with or without 10 μg/ml anti-CD44 blocking mAb KM201 at 4℃ for 10 minutes. The cells were then applied to the wells of a 96-well microtiter plate that had been coated with 4 μg/ml HA; adherent cells were measured by fluorescence spectrophotometry. Data are shown as percentage of adhesion (fluorescence intensity of cells adhered relative to that of input cells). n.s., not significant; $^{**}P<0.01$ versus untreated cells (ANOVA/Dunnett's test).

velocity did not change significantly (Fig. 6Ba). The rolling was completely inhibited with anti-CD44 blocking mAb KM201. (Fig. 6Bb). These results suggest that the dissociation of lipid rafts influences interactions between lymphocytes and HA tethered to endothelial cells.

Cholesterol depletion upregulates the HA-binding ability of CD44 in primary lymphocytes

To verify that the observations described above using a mouse T cell line have relevance for primary T cells, we tested the effect of cholesterol depletion on primary cultured cells isolated from the mouse spleen, which has abundant T cells. Resting primary $CD4^+$ T cells expressed CD44 at a high level, but did not exhibit HA-binding ability (Fig. 7). PMA- and ionomycin-activated $CD4^+$ T cells exhibited HA-binding ability with an increase in surface CD44 level. Treatment of the activated cells with MβCD (5 mM for 1 hour) upregulated their HA-binding, without altering their surface expression of CD44. HA binding was inhibited with anti-CD44 blocking mAb KM201. These results indicate that our observations of BW5147 T cells are applicable to primary T lymphocytes.

Next, we examined the lipid raft and rolling properties of primary T cells. The T cells were isolated by negative selection from resting spleen cells with 80.4% purity, as evaluated by staining of the pan-T cell marker CD3 (Fig. 8A). Activated T cells were also enriched as evaluated by staining of another T cell marker CD4 instead of CD3, since CD3 was internalized upon activation with PMA and ionomycin. Using these T cell-enriched fractions, we examined whether lipid rafts become dissociated in activated T cells by ultracentrifugation DRM analysis. Resting and activated T cell-enriched fractions were treated with MβCD (5 mM) or left untreated for 1 hour, lysed with Triton X-100, and subjected to gradient centrifugation analysis. As shown in

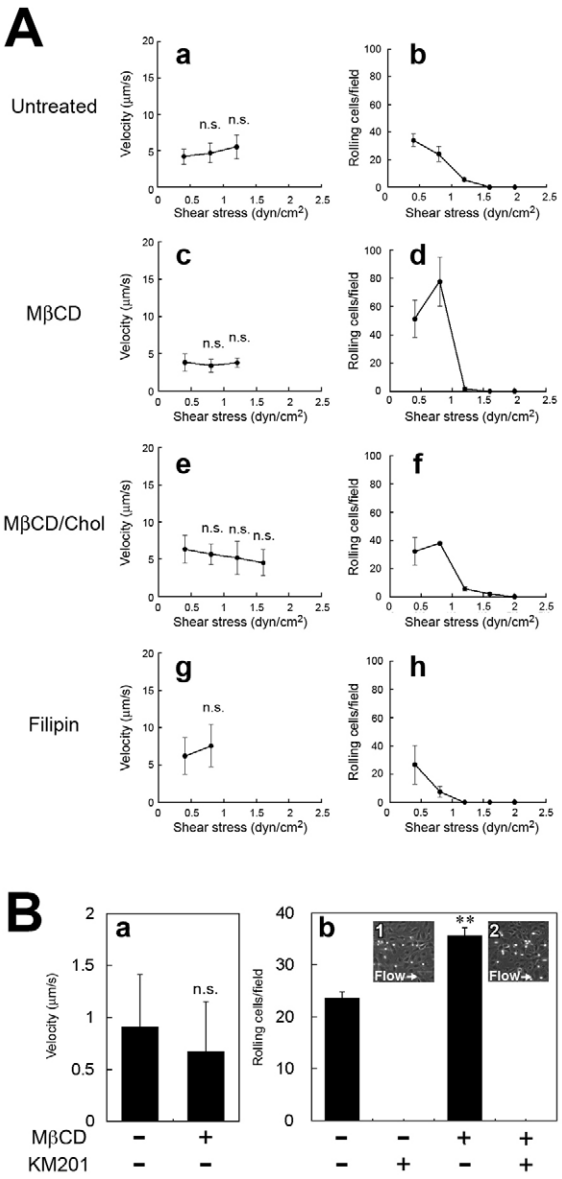

Fig. 6. Cholesterol depletion enhances cell rolling on HA under flow conditions. (**A**) Rolling on HA-coated substrate. BW5147 T cells were left untreated (Aa,Ab), MβCD-treated (5 mM for 1 hour; Ac,Ad), cholesterol-replenished (*MβCD/Chol*; Ae,Af) or filipin-treated (2 μg/ml for 1 hour; Ag,Ah) and then applied continuously to capillary tubes whose inner surface had been coated with HA. The average rolling velocity (Aa,Ac,Ae,Ag) and the number of rolling cells (Ab,Ad,Af,Ah) at wall shear stresses of 0.4, 0.8, 1.2, 1.6 or 2 dyn/cm^2 were determined as described in Materials and Methods. (**B**) Rolling on endothelial cells. BW5147 T cells treated with MβCD (5 mM for 1 hour) or left untreated were applied to SVEC4-10 endothelial cell monolayers equipped with a parallel plate flow chamber at a wall shear stress of 0.4 dyn/cm^2. For inhibition experiments, BW5147 T cells were incubated with 10 μg/ml anti-CD44 blocking mAb KM201 for 10 minutes prior to infusion to the chamber. Insets 1 and 2 show representative images captured from the flow assay with untreated and MβCD-treated BW5147 T cells, respectively. n.s., not significant; $^{**}P<0.01$ versus untreated cells.

Fig. 8B, a small fraction of the CD44 was found in the low density fraction (raft fraction) in both resting T cells and activated T cells, while CD44 was clearly lost from the low

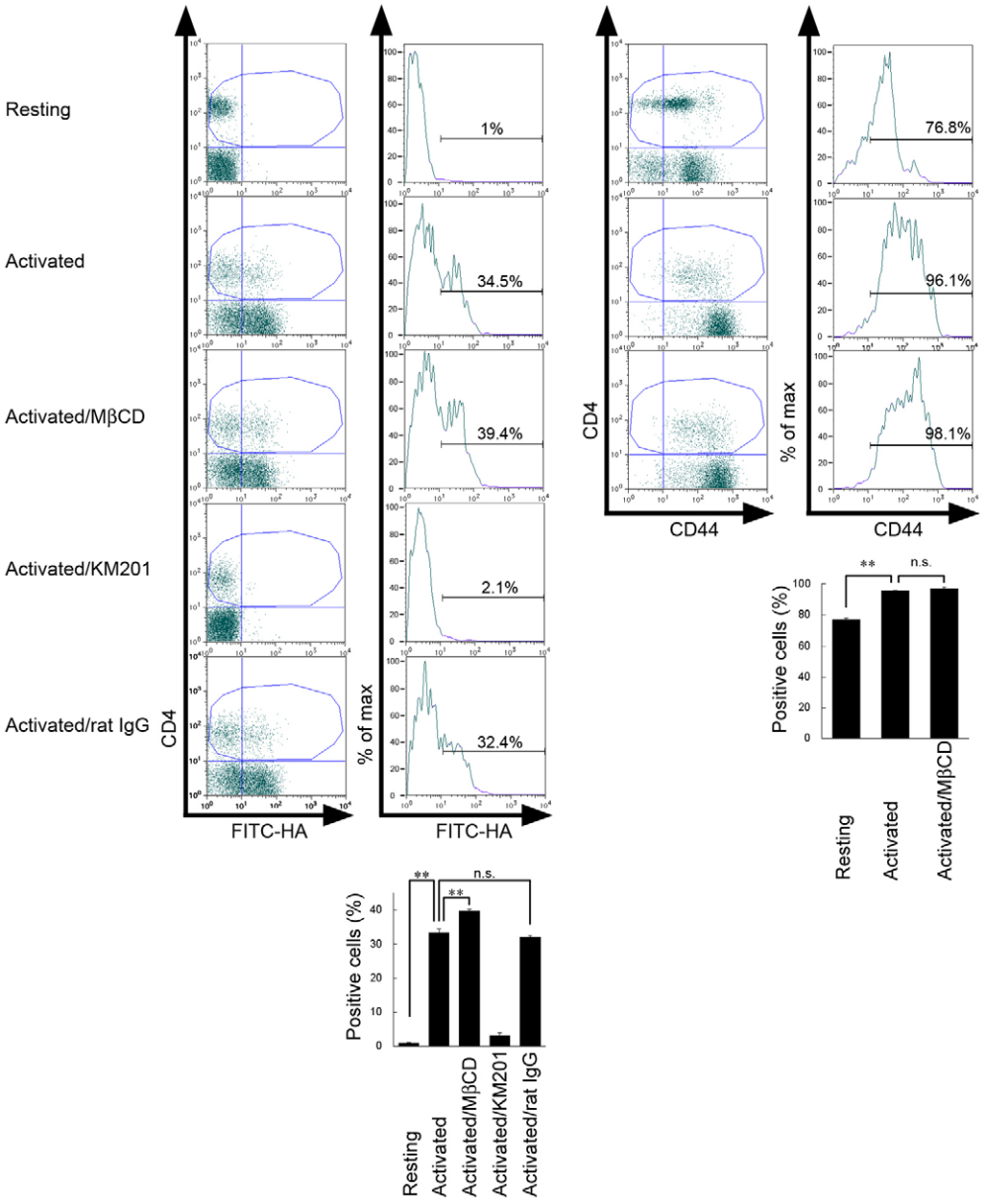

Fig. 7. MβCD enhances the HA-binding ability of CD44 in primary T cells. Resting mouse spleen cells or PMA- and ionomycin-activated spleen cells treated with or without 5 mM MβCD for 1 hour were co-stained with PE-conjugated anti-CD4 mAb and FITC–HA (left dot plots) or with PE-conjugated anti-CD4 mAb and FITC-conjugated anti-CD44 mAb (right dot plots), and then analyzed by two-color flow cytometry. The CD4-positive population was circled in each dot plot. For blocking experiments, activated spleen cells were treated with anti-CD44 blocking mAb KM201 or control rat IgG prior to staining. Histograms show the FITC–HA binding profiles (left) or CD44 level profiles (right) of the CD4-positive population. Percentages of gated cells are indicated. Bar graphs show the percentage of FITC–HA-positive (left) or CD44-positive (right) cells within CD4-positive populations. Data are presented as mean ± s.d. of triplicate determinations. n.s., not significant; $^{**}P<0.01$ (Student's *t*-test).

density fraction after cholesterol depletion with MβCD. The cellular cholesterol content did not exhibit significant difference between resting T cells and activated T cells (Fig. 8C). Finally, we tested whether the isolated primary T cells exhibit rolling adhesion on HA (Fig. 8D). While activated T cells did not interact with HA-coated surface under the flow condition tested, treatment of the activated T cells with MβCD induced rolling interaction with HA-coated surface at wall shear stresses of 0.4 and 0.8 dyn/cm^2 with unchanged average velocity.

Discussion

A number of reports have shown that CD44 is present in cholesterol-enriched lipid raft microdomains in various cell types including T cells (Ilangumaran et al., 1998; Gómez-Móuton et al., 2001; Oliferenko et al., 1999; Seveau et al., 2001; Pierini et al., 2003; Bourguignon et al., 2004). However, the functional significance of CD44 localization in the lipid rafts had been largely unknown. This study demonstrated the functional significance of this association in T cell adhesion properties. We demonstrated in the present study that cellular cholesterol modulates the HA-binding ability of CD44. Using BW5147 T cells, which express CD44 with HA-binding ability, we showed that cholesterol depletion induced with MβCD upregulates both the HA-binding ability of CD44 (Fig. 1) and the loss of CD44 from detergent-insoluble fractions (Fig. 3). We also found that cholesterol oxidation and sequestration upregulate CD44's HA-binding ability (Fig. 2), suggesting that the lipid rafts modulate CD44 function. MβCD also induced the binding of HA to CD44 expressed in primary T cells (Fig. 7). Untreated BW5147 T cells exhibit substantial HA-binding, whereas resting primary T cells do not. Thus the experiments using BW5147 T cells in the present study may be closely related to the enhancement of HA-binding ability rather than to the initial CD44 activation event.

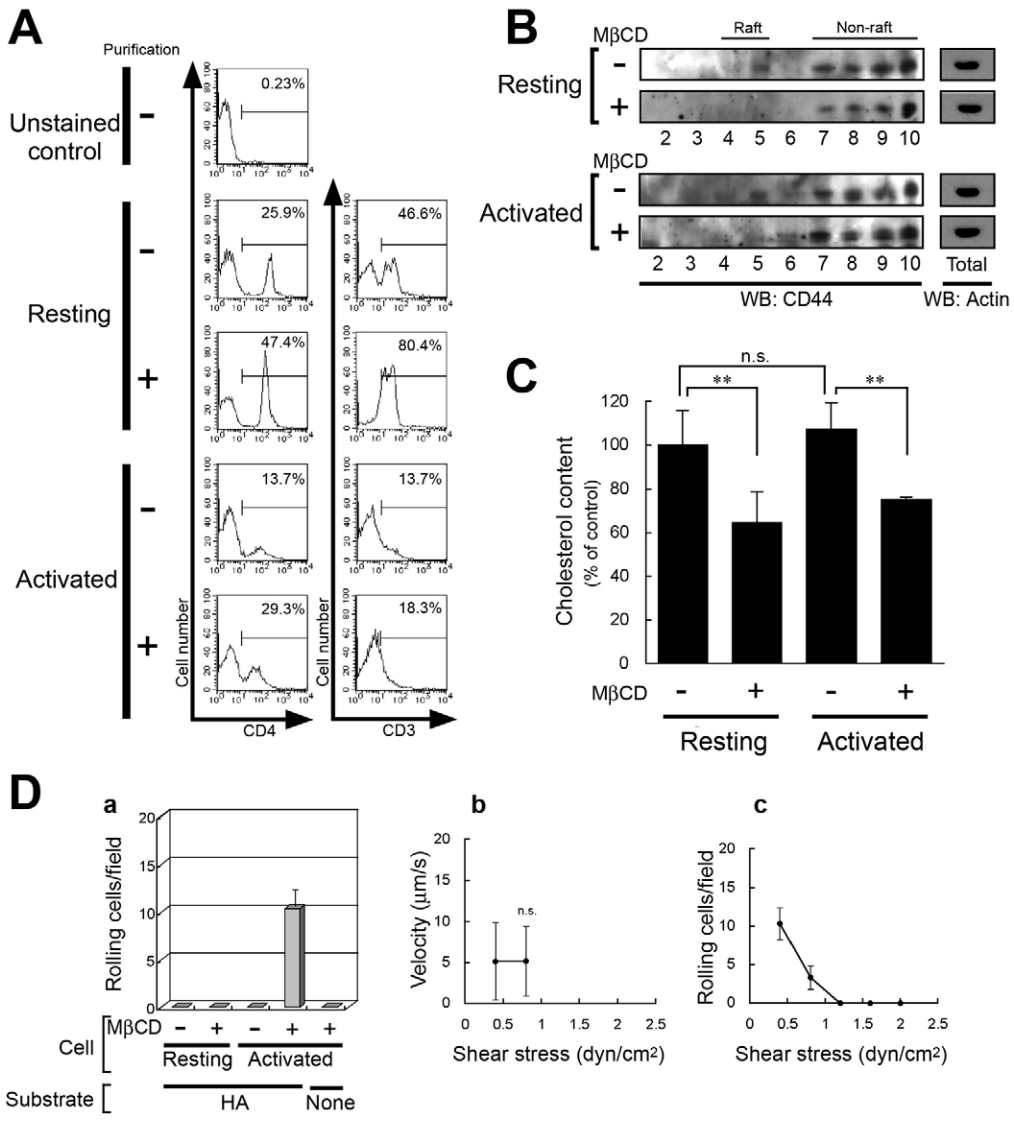

Fig. 8. MβCD induces rolling of primary T cells on HA under flow conditions. (**A**) Purification of splenic T cells. T cells were purified from resting mouse spleen cells or PMA- and ionomycin-activated spleen cells using a T cell column, and incubated with PE-conjugated anti-CD4 mAb or PE-conjugated anti-CD3 mAb. Staining of unpurified cells (−) and purified cells (+) was detected and analyzed by flow cytometry. Percentages of gated cells are indicated. (**B**) DRM fractionation of T cells. Purified resting T cells or activated T cells were treated with 5 mM MβCD or left untreated for 1 hour. Cells were then lysed in TNE buffer containing 0.5% Triton X-100 and the lysate was subjected to gradient centrifugation as described in Materials and Methods. Each fraction was analyzed by western blotting using anti-CD44 mAb IM7. β-Actin in each total cell lysate was detected as a loading control. (**C**) Changes in cellular cholesterol content after treatment with 5 mM MβCD for 1 hour. (**D**) Rolling of T cells on HA under flow conditions. Purified resting T cells or activated T cells were treated with 5 mM MβCD or left untreated for 1 hour and then applied continuously to capillary tubes whose inner surface had been coated with or without HA. The number of rolling cells at a wall shear stress of 0.4 dyn/cm^2 (Da) was determined as described in Materials and Methods. The average rolling velocity (Db) and the number of rolling cells (Dc) of activated T cells treated with MβCD were determined at wall shear stresses of 0.4, 0.8, 1.2, 1.6 or 2 dyn/cm^2 on HA. n.s., not significant; $^{**}P<0.01$ (Student's *t*-test).

The association of CD44 with lipid rafts is mediated by CD44's transmembrane region, which comprises 23 hydrophobic amino acids and a cysteine residue, and not by the cytoplasmic region (Perschl et al., 1995). Thankamony and Knudson reported that the cysteine residue in the transmembrane region, Cys^{286}, could become palmitoylated and the palmitoylation is required for association of CD44 to lipid rafts (Thankamony and Knudson, 2006). Cys^{286} seems to be involved in the upregulation of HA-binding ability of CD44 and the formation of CD44 covalent dimers upon PMA stimulation (Liu and Sy, 1997). In addition, Li et al. reported that CD44 in BW5147 T cells forms noncovalent self-association that is mediated by the transmembrane region of CD44 (Li et al., 1998). However, our experiments with a non-reducing PAGE or a chemical cross-linker bis(sulfosuccinimidyl)suberate failed to detect CD44 dimers upon cholesterol depletion and sequestration with MβCD and filipin, respectively (supplementary material Fig. S6). These results suggest that membrane cholesterol may modulate the HA-binding ability of CD44 through a mechanism different from that by PMA.

Although how CD44's ligand-binding ability is upregulated upon cholesterol depletion remains to be resolved, the results presented in this study support a hypothesis that the localization of CD44 in lipid rafts is perturbed when the raft is disrupted by cholesterol depletion/sequestration; the resulting increase in CD44 mobility in the membrane allows it to gain HA-binding avidity. The hypothesis is also supported by the observation that the lateral mobility of CD44 on the cell membrane was significantly enhanced when membrane cholesterol was depleted with MβCD (Oliferenko et al., 1999). Alternatively, one may raise the possibility that the membrane microenvironment may regulate the CD44's affinity to HA through conformational changes. The crystal structure of the mouse CD44–HA complex reveals two conformational forms of CD44 that differ in the orientation of a crucial HA-binding residue (Banerji et al., 2007). This conformational difference may provide a mechanism for the switching between low- and high-affinity binding states that have been observed in resting and activated lymphocytes, respectively (Lesley et al., 1993).

It has been reported that CD44 on the surface of cancer cells is prone to be shed upon stimulation by factors in the tumor environment, such as HA oligosaccharides (Sugahara et al., 2003;

Murai et al., 2004b; Sugahara et al., 2006) and epidermal growth factor (Murai et al., 2006). CD44 shedding also occurs upon cholesterol depletion from cancer cells (Murai et al., 2011). In the case of T cells, however, CD44 does not seem to be shed intensely upon MβCD treatment, since no detectable soluble CD44 was found after treatment with MβCD (supplementary material Fig. S4).

The control of adhesion properties of lymphocytes in vasculature is critical for immune response, and previous results showed that activation of lymphocytes increased the rolling frequency mediated by CD44–HA interactions (DeGrendele et al., 1996). Our results showing that cholesterol depletion increased the rolling frequency (Fig. 6), extend these findings by suggesting that lipid rafts are involved in the regulation of CD44-mediated rolling adhesion. In contrast to the rolling frequency, the rolling velocity was not changed upon cholesterol manipulation (Fig. 6), suggesting that CD44's residence in lipid rafts is not important for maintaining rolling adhesion under flow. These observations are consistent with L-selectin-mediated rolling, for which the topographical localization of L-selectin in microvilli was found to be important for enhancement of rolling frequency, but not to be a determinant of rolling velocity (von Andrian et al., 1995). The previous study showed that the CD44 expressed in L1-2 pre-B cells was mainly found on the cell body, and was not associated with microvilli (von Andrian et al., 1995). In contrast, ASEM analysis revealed that CD44 was displayed over the entire cell surface of BW5147 T cells (Fig. 4), and CD44 localized in DRMs that include lipid rafts was lost after cholesterol depletion (Fig. 3). The results in the present study raise a possibility that the CD44's cholesterol-dependent allocation to lipid rafts may regulate the frequency of the CD44-dependent rolling adhesion. The CD44-mediated rolling velocity seems to be almost constant within the range of physiological shear stress (Fig. 6), suggesting that an automatic breaking system may stabilize the CD44-mediated rolling adhesion as in the L-selectin-mediated rolling (Chen and Springer, 1999).

We purified T cells from mouse spleen cells, analyzed the lipid rafts of resting and activated T cells by ultracentrifugation analysis, and found that activated T cells still have lipid rafts that contain a portion of CD44 (Fig. 8B). These results indicate that lipid rafts are not dissociated in activated T cells, and that the CD44's dissociation from lipid rafts is not required for the CD44's transition from its inactive state expressed in resting T cells to the active state expressed in activated T cells, but plays a role in further upregulation of HA binding of the already-activated CD44. These results suggest that the well-known and newly-identified stimuli, i.e. PMA/ionomycin and MβCD, respectively, function at the different stages during CD44 activation. Additionally, we performed shear flow assay using purified T cells (Fig. 8D). The results demonstrate that PMA/ionomycin-activated T cells did not roll on HA, while the activated T cells exhibited rolling upon cholesterol depletion. Considering the fact that *in vivo*-activated T cells exhibit rolling on HA (DeGrendele et al., 1996), the two types of *in vitro* stimuli, PMA/ionomycin and MβCD, might be important with physiological relevance in terms of PKC-mediated signal transduction and cholesterol-mediated raft regulation, respectively.

In conclusion, we have presented evidence that lipid rafts modulate CD44's binding ability for HA. Our findings provide novel insight into how the adhesion of T cells is regulated under blood flow.

Materials and Methods

Reagents

HA from rooster comb, MβCD, cholesterol, cholesterol oxidase [EC 1.1.3.6] from *Brevibacterium sp.*, filipin III from *Streptomyces filipinensis*, PMA, and ionomycin were purchased from Sigma. Rat anti-mouse CD44 mAb IM7.8.1 was purchased from BD Biosciences. PE-conjugated hamster anti-mouse CD3ε mAb and FITC-conjugated IM7.8.1 were purchased from BioLegend (San Diego, CA). PE-conjugated rat anti-mouse CD4 mAb was purchased from Beckman Coulter. FITC–HA (180 and 1300 kDa) was purchased from PG Research (Tokyo, Japan). Biotin-conjugated cholera toxin subunit B (CTxB) and FITC-conjugated goat anti-rat IgG were purchased from Invitrogen. Nonogold (1.4 nm)- and Alexa Fluor 488-conjugated goat anti-rat IgG and GoldEnhance-EM were purchased from Nonoprobes, Inc. (Yaphank, NY). Anti-β-actin mAb was purchased from Santa Cruz Biotechnology (Santa Cruz, CA).

Cell culture

The mouse T lymphocyte cell line BW5147, obtained from ATCC, was maintained in RPMI 1640 medium (Sigma) supplemented with 10% FCS, 100 units/ml penicillin and 100 μg/ml streptomycin, and incubated at 37℃ in an atmosphere containing 5% CO_2. Primary spleen cells were obtained from C57/BL6 mice (Japan SLC, Hamamatsu, Japan) and activated *in vitro* by incubation with 3 ng/ml PMA and 1.5 μg/ml ionomycin for 24 hours at room temperature and subsequently for 20 hours at 37℃ in an atmosphere containing 5% CO_2. T cells were isolated from spleen cells by negative selection using T cell enrichment column (R&D Systems) according to the manufacturer's instruction. The mice were treated in accordance with the guidelines of the Animal Research Committee of the University of Shizuoka. The mouse lymph node cell line SVEC4-10, obtained from ATCC, was maintained in DMEM (Sigma) supplemented with 10% FCS, 100 units/ml penicillin and 100 μg/ml streptomycin, and incubated at 37℃ in an atmosphere containing 5% CO_2.

Manipulation of cellular cholesterol

For cholesterol depletion, cells were washed twice with serum-free medium and then incubated with 2.5–10 mM MβCD. For cholesterol replenishment, the cells were further treated for 30 minutes with a 0.3 mM cholesterol–MβCD inclusion complex (Klein et al., 1995). To oxidize the membrane cholesterol, cells were incubated with 0.5 U/ml cholesterol oxidase for 1 hour at 37℃. To perturb the lipid rafts, cells were treated with 2 μg/ml filipin for 1 hour. All the reagents were diluted in serum-free RPMI 1640 medium. Cellular cholesterol content was assayed spectrophotometrically using an Amplex Red cholesterol assay kit (Invitrogen).

Flow cytometry

To measure HA binding, BW5147 T cells were incubated on ice with or without 2 μg/ml FITC–HA (180 kDa) for 1 hour. To detect cell-surface CD44, cells were incubated on ice with 1 μg/ml anti-CD44 mAb IM7 or normal rat IgG, and then stained with FITC-conjugated goat anti-rat IgG. In experiments with primary spleen cells and isolated T cells, 2 μg/ml FITC–HA (1300 kDa) and 1 μg/ml FITC-conjugated IM7 was used for determination of HA binding and CD44 level, respectively. For staining of T cell markers, cells were incubated with 0.2 μg/ml PE-conjugated anti-CD3ε mAb or with 0.2 μg/ml PE-conjugated anti-CD4 mAb. Samples were analyzed using a FACS Calibur (BD Biosciences) with CELLQuest research software (BD Biosciences) and FlowJo software (Tree Star, OR).

Isolation of DRM fractions

DRM fractions were prepared as previously described with minor modifications (Gómez-Móuton et al., 2001). Briefly, BW5147 T cells or purified T cells were treated with MβCD (5 mM, 1 hour) or left untreated, and lysed in TNE buffer [25 mM Tris-HCl pH 7.4, 150 mM NaCl, 5 mM EDTA, and a protease inhibitor mixture (Roche Applied Science)] containing 0.5% (v/v) Triton X-100 for 20 minutes on ice. Subsequently, the lysate was brought to 40% (w/v) iodixanol using OptiPrep (Axis-Shield, Oslo, Norway) and overlaid with 1 ml each of 35, 30, 25 and 20% iodixanol in TNE buffer, and finally with 3.5 ml TNE buffer. The gradients were centrifuged at 250,000×***g*** with a SW41 rotor for 16 hours at 4℃. Fractions (1 ml each) were collected from the top, and equal amounts of each fraction were analyzed by western blotting. The lipid raft marker GM1 was detected by dot blot analysis using biotinylated CTxB and HRP-conjugated streptavidin (Invitrogen).

Atmospheric scanning immunoelectron microscopy

Affinity-labeling with gold conjugates and imaging with recently developed ASEM were performed as described previously (Murai et al., 2011). In brief, cells were cultured on a SiN film of 100 nm in thickness, in RPMI supplemented with

10% FCS, in a 5% CO_2 atmosphere at 37℃. The cells were treated with 5 mM MβCD for 1 hour and fixed with 4% paraformaldehyde in PBS at room temperature for 10 minutes. For the detection of CD44 on the cell surface, the cells were incubated with 1% skim milk/PBS for 30 minutes, with IM7 mAb for 1 hour, and then with Alexa Fluor 488- and Nanogold-conjugated goat anti-rat IgG for 30 minutes. The Nanogold signal was enhanced using GoldEnhance-EM at room temperature for 5 minutes. The labeled cells in 10 mg/ml ascorbic acid solution were directly observed by ASEM.

Static cell adhesion assay

Cells were labeled with 5 μM 5-chloromethylfluorescein diacetate (CMFDA) (Life Technologies) for 30 minutes at 37℃ and were otherwise untreated, MβCD-treated (5 mM for 1 hour), cholesterol-replenished, or filipin-treated (2 μg/ml for 1 hour). They were then rinsed and resuspended in PBS in the presence or absence of 10 μg/ml rat anti-mouse CD44 mAb KM201 (ATCC #TIB-240), incubated at 4℃ for 10 minutes, and then aliquotted into a 96-well microtiter plate (1×10^5 cells/well; Smilon H, Sumitomo Bakelite, Tokyo, Japan) that had been coated with 4 μg/ml HA and subsequently blocked with 5% BSA/PBS. After incubation on ice for 40 minutes, the wells were filled with PBS. The plate was then inverted, and kept upside-down for 30 seconds. After the unbound cells were removed by gentle aspiration, 1% Nonidet P-40/PBS was added to each well, and the plate was read in a fluorescence spectrophotometer at 485 nm excitation and 538 nm emission.

Shear flow assay

The capillary shear flow assay was performed as previously described (Murai et al., 2004a). Briefly, BW5147 T cells or primary T cells that had been subjected to cholesterol manipulation or were untreated, were rinsed and resuspended in prewarmed RPMI 1640 medium at 1×10^6 cells/ml. The cell suspension was then transfused through a capillary tube (Drummond Scientific, Broomall, PA), the inner surface of which had been coated with 1 mg/ml HA and subsequently blocked with 5% BSA, at a wall shear stress ranging from 0.4 to 2 dyn/cm^2 using a syringe pump (Harvard Apparatus, South Natick, MA). The number of rolling cells and their rolling velocity were analyzed by video microscopy using ImageJ software.

For shear flow assay on endothelial cells, monolayers of SVEC4-10 endothelial cells cultured in 40-mm dish (Iwaki Glass, Japan) were used at confluence. After incubation with 10 ng/ml mouse tumor-necrosis factor-α (R&D Systems) for 4 hours, the dishes were equipped with a parallel plate flow chamber (Glycotech Inc., Gaithersburg, MD). BW5147 T cells or primary T cells that had been incubated with or without MβCD were resuspended in prewarmed RPMI 1640 medium at 1×10^6 cells/ml, and introduced into the flow chamber at a wall shear stress ranging from 0.4 to 2 dyn/cm^2 using a syringe pump according to the manufacturer's instructions. For inhibition experiments, BW5147 T cells were incubated with 10 μg/ml anti-CD44 blocking mAb KM201 for 10 minutes prior to infusion to the chamber.

Statistical analysis

Student's *t*-test or ANOVA followed by post hoc Dunnett's test was used to determine statistical significance between experimental groups. All the results were expressed as means ± s.d.

Author contributions

T.M. designed the project, performed experiments, analysed data and wrote the manuscript; C.S. and M. Sato performed experiments and analysed data; H.N. and M. Suga provided expertise; K.M. analysed and discussed the data; H.K. designed and performed experiments, analysed data and contributed to the preparation of the manuscript.

Funding

This work was supported by a Grant-in-Aid from the Ministry of Education, Culture, Sports, Science, and Technology of Japan.

Supplementary material available online at
http://jcs.biologists.org/lookup/suppl/doi:10.1242/jcs.120014/-/DC1

References

Ariel, A., Lider, O., Brill, A., Cahalon, L., Savion, N., Varon, D. and Hershkoviz, R. (2000). Induction of interactions between CD44 and hyaluronic acid by a short exposure of human T cells to diverse pro-inflammatory mediators. *Immunology* **100**, 345-351.

Banerji, S., Wright, A. J., Noble, M., Mahoney, D. J., Campbell, I. D., Day, A. J. and Jackson, D. G. (2007). Structures of the Cd44-hyaluronan complex provide insight into a fundamental carbohydrate-protein interaction. *Nat. Struct. Mol. Biol.* **14**, 234-239.

Bonder, C. S., Clark, S. R., Norman, M. U., Johnson, P. and Kubes, P. (2006). Use of CD44 by CD4+ Th1 and Th2 lymphocytes to roll and adhere. *Blood* **107**, 4798-4806.

Bourguignon, L. Y. W., Singleton, P. A., Diedrich, F., Stern, R. and Gilad, E. (2004). CD44 interaction with Na^+-H^+ exchanger (NHE1) creates acidic microenvironments leading to hyaluronidase-2 and cathepsin B activation and breast tumor cell invasion. *J. Biol. Chem.* **279**, 26991-27007.

Brown, K. L., Maiti, A. and Johnson, P. (2001). Role of sulfation in CD44-mediated hyaluronan binding induced by inflammatory mediators in human $CD14^+$ peripheral blood monocytes. *J. Immunol.* **167**, 5367-5374.

Chen, S. and Springer, T. A. (1999). An automatic braking system that stabilizes leukocyte rolling by an increase in selectin bond number with shear. *J. Cell Biol.* **144**, 185-200.

Clark, R. A., Alon, R. and Springer, T. A. (1996). CD44 and hyaluronan-dependent rolling interactions of lymphocytes on tonsillar stroma. *J. Cell Biol.* **134**, 1075-1087.

DeGrendele, H. C., Estess, P., Picker, L. J. and Siegelman, M. H. (1996). CD44 and its ligand hyaluronate mediate rolling under physiologic flow: a novel lymphocyte-endothelial cell primary adhesion pathway. *J. Exp. Med.* **183**, 1119-1130.

DeGrendele, H. C., Estess, P. and Siegelman, M. H. (1997). Requirement for CD44 in activated T cell extravasation into an inflammatory site. *Science* **278**, 672-675.

English, N. M., Lesley, J. F. and Hyman, R. (1998). Site-specific de-*N*-glycosylation of CD44 can activate hyaluronan binding, and CD44 activation states show distinct threshold densities for hyaluronan binding. *Cancer Res.* **58**, 3736-3742.

Fessler, M. B. and Parks, J. S. (2011). Intracellular lipid flux and membrane microdomains as organizing principles in inflammatory cell signaling. *J. Immunol.* **187**, 1529-1535.

Firan, M., Dhillon, S., Estess, P. and Siegelman, M. H. (2006). Suppressor activity and potency among regulatory T cells is discriminated by functionally active CD44. *Blood* **107**, 619-627.

Gómez-Móuton, C., Abad, J. L., Mira, E., Lacalle, R. A., Gallardo, E., Jiménez-Baranda, S., Illa, I., Bernad, A., Mañes, S. and Martínez-A, C. (2001). Segregation of leading-edge and uropod components into specific lipid rafts during T cell polarization. *Proc. Natl. Acad. Sci. USA* **98**, 9642-9647.

Ilangumaran, S. and Hoessli, D. C. (1998). Effects of cholesterol depletion by cyclodextrin on the sphingolipid microdomains of the plasma membrane. *Biochem. J.* **335**, 433-440.

Ilangumaran, S., Briol, A. and Hoessli, D. C. (1998). CD44 selectively associates with active Src family protein tyrosine kinases Lck and Fyn in glycosphingolipid-rich plasma membrane domains of human peripheral blood lymphocytes. *Blood* **91**, 3901-3908.

Katoh, S., Zheng, Z., Oritani, K., Shimozato, T. and Kincade, P. W. (1995). Glycosylation of CD44 negatively regulates its recognition of hyaluronan. *J. Exp. Med.* **182**, 419-429.

Kawashima, H. (2006). Roles of sulfated glycans in lymphocyte homing. *Biol. Pharm. Bull.* **29**, 2343-2349.

Kawashima, H., Petryniak, B., Hiraoka, N., Mitoma, J., Huckaby, V., Nakayama, J., Uchimura, K., Kadomatsu, K., Muramatsu, T., Lowe, J. B. et al. (2005). *N*-acetylglucosamine-6-*O*-sulfotransferases 1 and 2 cooperatively control lymphocyte homing through L-selectin ligand biosynthesis in high endothelial venules. *Nat. Immunol.* **6**, 1096-1104.

Klein, U., Gimpl, G. and Fahrenholz, F. (1995). Alteration of the myometrial plasma membrane cholesterol content with β-cyclodextrin modulates the binding affinity of the oxytocin receptor. *Biochemistry* **34**, 13784-13793.

Le Lay, S., Li, Q., Proschogo, N., Rodriguez, M., Gunaratnam, K., Cartland, S., Rentero, C., Jessup, W., Mitchell, T. and Gaus, K. (2009). Caveolin-1-dependent and -independent membrane domains. *J. Lipid Res.* **50**, 1609-1620.

Lesley, J., Hyman, R. and Kincade, P. W. (1993). CD44 and its interaction with extracellular matrix. *Adv. Immunol.* **54**, 271-335.

Lesley, J., Howes, N., Perschl, A. and Hyman, R. (1994). Hyaluronan binding function of CD44 is transiently activated on T cells during an in vivo immune response. *J. Exp. Med.* **180**, 383-387.

Levesque, M. C. and Haynes, B. F. (1999). TNFα and IL-4 regulation of hyaluronan binding to monocyte CD44 involves posttranslational modification of CD44. *Cell. Immunol.* **193**, 209-218.

Li, R., Walker, J. R. and Johnson, P. (1998). Chimeric CD4/CD44 molecules associate with CD44 via the transmembrane region and reduce hyaluronan binding in T cell lines. *Eur. J. Immunol.* **28**, 1745-1754.

Liu, D. and Sy, M.-S. (1997). Phorbol myristate acetate stimulates the dimerization of CD44 involving a cysteine in the transmembrane domain. *J. Immunol.* **159**, 2702-2711.

Maeshima, N., Poon, G. F. T., Dosanjh, M., Felberg, J., Lee, S. S. M., Cross, J. L., Birkenhead, D. and Johnson, P. (2011). Hyaluronan binding identifies the most proliferative activated and memory T cells. *Eur. J. Immunol.* **41**, 1108-1119.

Maiti, A., Maki, G. and Johnson, P. (1998). TNF-α induction of CD44-mediated leukocyte adhesion by sulfation. *Science* **282**, 941-943.

McGookey, D. J., Fagerberg, K. and Anderson, R. G. W. (1983). Filipin-cholesterol complexes form in uncoated vesicle membrane derived from coated vesicles during receptor-mediated endocytosis of low density lipoprotein. *J. Cell Biol.* **96**, 1273-1278.

Murai, T., Sougawa, N., Kawashima, H., Yamaguchi, K. and Miyasaka, M. (2004a). CD44-chondroitin sulfate interactions mediate leukocyte rolling under physiological flow conditions. *Immunol. Lett.* **93**, 163-170.

Murai, T., Miyazaki, Y., Nishinakamura, H., Sugahara, K. N., Miyauchi, T., Sako, Y., Yanagida, T. and Miyasaka, M. (2004b). Engagement of CD44 promotes Rac

activation and CD44 cleavage during tumor cell migration. *J. Biol. Chem.* **279**, 4541-4550.

Murai, T., Miyauchi, T., Yanagida, T. and Sako, Y. (2006). Epidermal growth factor-regulated activation of Rac GTPase enhances CD44 cleavage by metalloproteinase disintegrin ADAM10. *Biochem. J.* **395**, 65-71.

Murai, T., Maruyama, Y., Mio, K., Nishiyama, H., Suga, M. and Sato, C. (2011). Low cholesterol triggers membrane microdomain-dependent CD44 shedding and suppresses tumor cell migration. *J. Biol. Chem.* **286**, 1999-2007.

Nishiyama, H., Suga, M., Ogura, T., Maruyama, Y., Koizumi, M., Mio, K., Kitamura, S. and Sato, C. (2010). Atmospheric scanning electron microscope observes cells and tissues in open medium through silicon nitride film. *J. Struct. Biol.* **169**, 438-449.

Ohmichi, Y., Hirakawa, J., Imai, Y., Fukuda, M. and Kawashima, H. (2011). Essential role of peripheral node addressin in lymphocyte homing to nasal-associated lymphoid tissues and allergic immune responses. *J. Exp. Med.* **208**, 1015-1025.

Oliferenko, S., Paiha, K., Harder, T., Gerke, V., Schwärzler, C., Schwarz, H., Beug, H., Günthert, U. and Huber, L. A. (1999). Analysis of CD44-containing lipid rafts: Recruitment of annexin II and stabilization by the actin cytoskeleton. *J. Cell Biol.* **146**, 843-854.

Perschl, A., Lesley, J., English, N., Hyman, R. and Trowbridge, I. S. (1995). Transmembrane domain of CD44 is required for its detergent insolubility in fibroblasts. *J. Cell Sci.* **108**, 1033-1041.

Pierini, L. M., Eddy, R. J., Fuortes, M., Seveau, S., Casulo, C. and Maxfield, F. R. (2003). Membrane lipid organization is critical for human neutrophil polarization. *J. Biol. Chem.* **278**, 10831-10841.

Rodal, S. K., Skretting, G., Garred, Ø., Vilhardt, F., van Deurs, B. and Sandvig, K. (1999). Extraction of cholesterol with methyl-β-cyclodextrin perturbs formation of clathrin-coated endocytic vesicles. *Mol. Biol. Cell* **10**, 961-974.

Rosen, S. D. (2004). Ligands for L-selectin: homing, inflammation, and beyond. *Annu. Rev. Immunol.* **22**, 129-156.

Rothberg, K. G., Ying, Y.-S., Kamen, B. A. and Anderson, R. G. W. (1990). Cholesterol controls the clustering of the glycophospholipid-anchored membrane receptor for 5-methyltetrahydrofolate. *J. Cell Biol.* **111**, 2931-2938.

Ruffell, B., Poon, G. F. T., Lee, S. S. M., Brown, K. L., Tjew, S.-L., Cooper, J. and Johnson, P. (2011). Differential use of chondroitin sulfate to regulate hyaluronan binding by receptor CD44 in Inflammatory and Interleukin 4-activated Macrophages. *J. Biol. Chem.* **286**, 19179-19190.

Seveau, S., Eddy, R. J., Maxfield, F. R. and Pierini, L. M. (2001). Cytoskeleton-dependent membrane domain segregation during neutrophil polarization. *Mol. Biol. Cell* **12**, 3550-3562.

Simons, K. and Ikonen, E. (1997). Functional rafts in cell membranes. *Nature* **387**, 569-572.

Skelton, T. P., Zeng, C., Nocks, A. and Stamenkovic, I. (1998). Glycosylation provides both stimulatory and inhibitory effects on cell surface and soluble CD44 binding to hyaluronan. *J. Cell Biol.* **140**, 431-446.

Springer, T. A. (1994). Traffic signals for lymphocyte recirculation and leukocyte emigration: the multistep paradigm. *Cell* **76**, 301-314.

Sugahara, K. N., Murai, T., Nishinakamura, H., Kawashima, H., Saya, H. and Miyasaka, M. (2003). Hyaluronan oligosaccharides induce CD44 cleavage and promote cell migration in CD44-expressing tumor cells. *J. Biol. Chem.* **278**, 32259-32265.

Sugahara, K. N., Hirata, T., Hayasaka, H., Stern, R., Murai, T. and Miyasaka, M. (2006). Tumor cells enhance their own CD44 cleavage and motility by generating hyaluronan fragments. *J. Biol. Chem.* **281**, 5861-5868.

Thankamony, S. P. and Knudson, W. (2006). Acylation of CD44 and its association with lipid rafts are required for receptor and hyaluronan endocytosis. *J. Biol. Chem.* **281**, 34601-34609.

von Andrian, U. H., Hasslen, S. R., Nelson, R. D., Erlandsen, S. L. and Butcher, E. C. (1995). A central role for microvillous receptor presentation in leukocyte adhesion under flow. *Cell* **82**, 989-999.